CYCLIC STRUT & TIE MODELLING OF SIMPLE REINFORCED CONCRETE STRUCTURES

Nicholas H T TO[1], Jason M INGHAM[2] And S SRITHARAN[3]

SUMMARY

The study reported in the current research paper represents an initial attempt to develop simple strut-and-tie model (stm) formation procedures, which allow the cyclic hysteretic response of reinforced concrete structures to be examined. An idealised uniaxial fibre model was firstly constructed to simulate the axial force-displacement characteristic of a combined concrete and steel reinforcing element. This model was subsequently employed as the top and bottom chord members in the later constructed stm. Nonlinear computer analysis of the newly developed stm was performed using drain-2dx. Analytical output was found to satisfactorily match the experimentally measured force-displacement response. However, several deficiencies of the model required further study.

INTRODUCTION

The strut and tie model (STM) is a discrete representation of stress fields developed in reinforced concrete structures subjected to external actions. Within the model, the actual compressive and tensile stress are separately represented by compression struts and tension ties respectively. These elements are joined together at nodal points, where curvature of actual stress trajectory concentrated.

In the recent past, STM has been substantially utilised in detailing and dimensioning of D-regions of reinforced concrete structures, where a linear stress-strain distribution is invalid. These structures include deep beams, shear walls, corbels and beam-column joints. Although application of this methodology has predominantly been concentrated in the previously stated structural components, this analytical technique is identically applicable to the B-region where sectional linearity of the stress-strain distribution prevails.

Accordingly, as firstly advocated by Schlaich et al. [1987], the emerging design strategy of STM for both D- and B- regions provides a unified design approach, resulting in a consistent design standard for all structural types. A typical example illustrating this concept is depicted in Fig.1, where a STM of a portal bridge frame is constructed for monotonic response analysis.

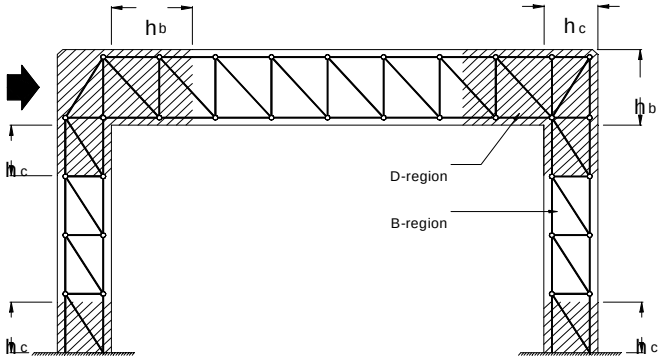

Figure 1. STM of a portal bridge bent.

While the expected goal of the current research project is to incorporate the philosophy of unified design strategy into the STM formation procedures, which allows the cyclic hysteretic response of various reinforced concrete structural types to be examined when subjected to time history earthquake loading. An initial research progress made in

[1] *Ph.D. Student, Department of Civil and Resources Engineering, University of Auckland, New Zealand*
[2] *C&CA Lecturer, Department of Civil and Resources Engineering, University of Auckland, New Zealand*
[3] *Assistant Professor, Department of Civil and Construction Engineering, Iowa State University, USA.*

this direction was reported in the current research paper. Within the study, an idealised uniaxial fibre model was firstly constructed in order to simulate the combined axial characteristic of concrete and steel reinforcement when subjected to tension and compression. A general approach was subsequently proposed to determine the appropriate position, and effective size and strength of STM members composed of the uniaxial fibre model. Drain-2DX was employed to perform nonlinear analysis for the newly developed STM of simple reinforced concrete cantilever beams. Force displacement hysteretic response were compared to experimental results for justification.

IDEALISED UNIAXIAL FIBRE MODEL

Seventeen reinforced concrete prisms were tested under axial cyclic action by Tjokrodimuljo [1985] in the University of Auckland. The aim of the experiment was to investigate the cyclic hysteretic response of the top or bottom zone of a beam or column subjected to the repeated tension and compression in the reversed flexural cyclic loading. In the direct extension of the experiment, an idealised uniaxial fibre model as shown in Fig. 2 was developed for the top and bottom chord members of the later constructed STM. This model consists of two uniaxial elements arranged in tandem, namely a link element and a truss element. By developing a gap, the link element is employed to perform as a concrete member which carries no tension force. The truss element acts as a typical reinforcing steel bar capable of supporting both tension and compression forces. The stress-strain characteristics of both elements are represented with bilinear approximations as shown in Fig. 3a & 3b, while Fig. 3c shows the typical cyclic stress-strain response of the combined material types.

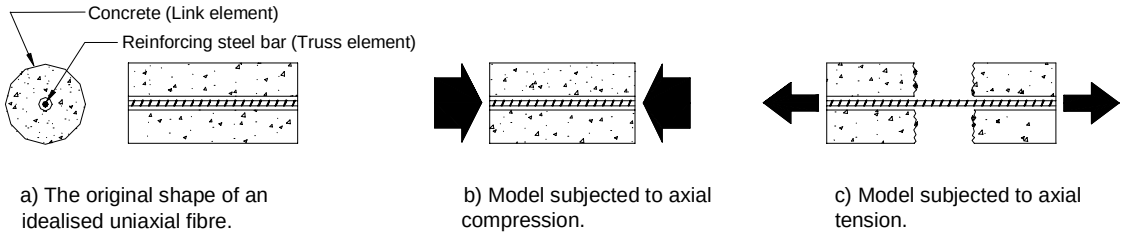

Figure 2. Idealised uniaxial fibre model.

The equation suggested by Eurocode 2[1991] was adopted to compute the elasticity modulus of concrete, E_c. This equation was preferred since it was believed to best predict the probable value rather than a suitable design value:

$$E_c = 9.5(f_c' + 8)^{1/3} \quad \text{GPa} \tag{1}$$

Experimental results [Tjokrodimuljo, 1985] show that a 15% reduction of concrete compressive strength in the reinforced concrete prisms if the steel was previously subjected to high inelastic strain. Consequently, the effective concrete compressive strength, f_d, was taken as $0.85f'_c$, see Fig. 3a(ii) in the uniaxial fibre model, to take account of such damage effects. The computation of a bilinear approximation for the steel truss element is straightforward. The commonly assumed value [NZS 3101:1995] for steel elastic modulus, E_s = 200GPa, and a strain hardening ratio of 0.5% were assigned.

Once the bilinear stress-strain approximations were defined, the link and truss elements were assembled together according to the configuration of reinforced concrete prisms tested in the experiment. The nonlinear load displacement characteristic of the uniaxial fibre model was analysed using Drain-2DX and the results found to agree well with experimental observations, see Fig. 3c.

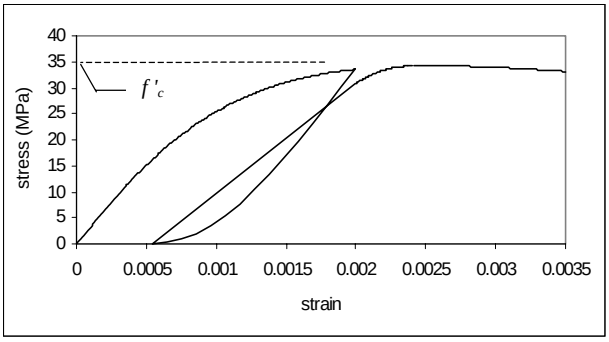

a i) – Typical cyclic stress-strain relationship of concrete element.

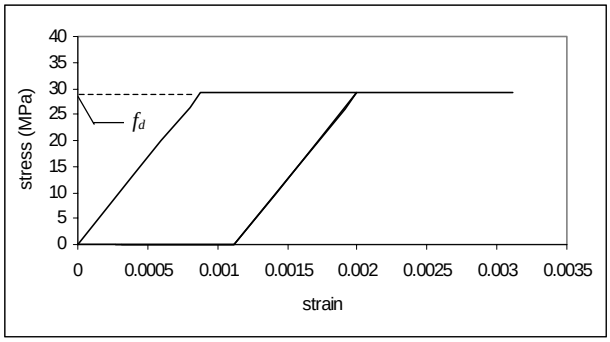

a ii) – Bilinear cyclic stress-strain approximation of concrete element.

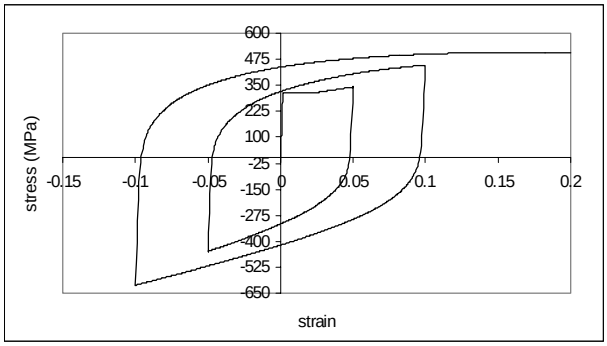

b i) – Typical reversed cyclic stress-strain relationship of steel reinforcement.

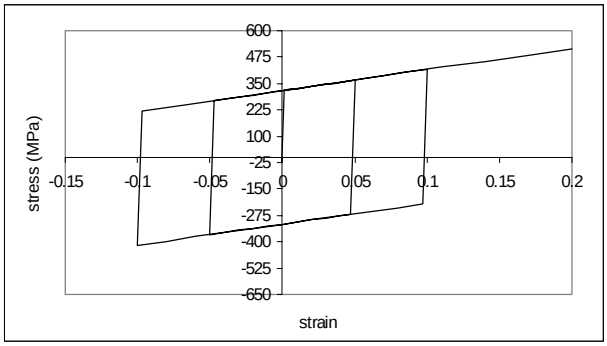

b i) – Bilinear reversed cyclic stress-strain approximation of steel reinforcement.

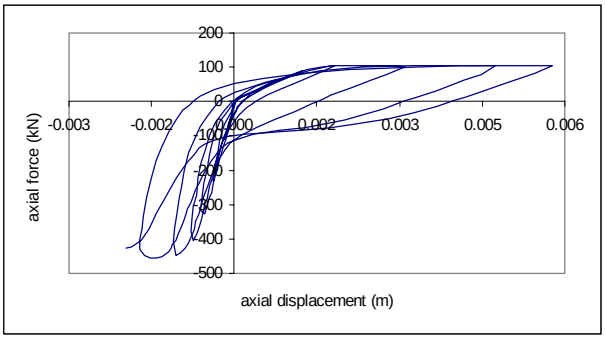

c i) – Experimental data for the combined force-displacement response of concrete and reinforcing steel.

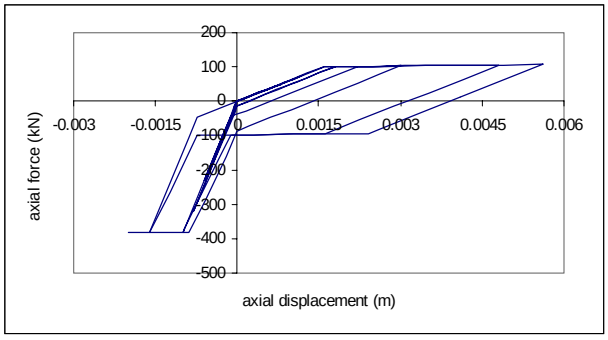

c ii) – Nonlinear analytical outputs of the uniaxial fibre model.

Figure 3. Axial cyclic response of concrete and reinforcing steel members.

STRUT AND TIE MODELLING

If the compression steel reinforcement of the beam shown in Fig. 4a was previously subjected to high inelastic tensile strain, it is necessary for the steel to yield in compression before the flexural cracks can close and allow the concrete to carry any appreciable compressive stress. However the fully closure of flexural cracks is not possible due to the development of truss mechanism and also due to the dislocated aggregate acting as a wedge across the cracks [Douglas, 1995]. Hence the compression reinforcement will carry most of the compression force and internal lever arm of beam section becomes the distance between force centroids of top and bottom steel reinforcement. Accordingly, the STM top and bottom chord members in the later constructed model were located in the corresponding steel centroid.

In order to conveniently formulate the STM member size, the ratio of cracked elastic neutral axis depth to total section depth, η, was computed for a doubly reinforced beam section, see Fig. 4a. It was done by assuming that compression and tension steel reinforcement are respectively located at a distance of 10% and 90% of the total section depth, h, measured from the upper edge of the section. This assumption is acceptable for the commonly found section in the beam designed for seismic loading where the top and bottom longitudinal steel

reinforcements have minimal cover to the corresponding edges of the section. Results are plotted in Fig. 4b for various concrete compressive strength, f'_c, and the top to bottom steel reinforcement ratio, ω.

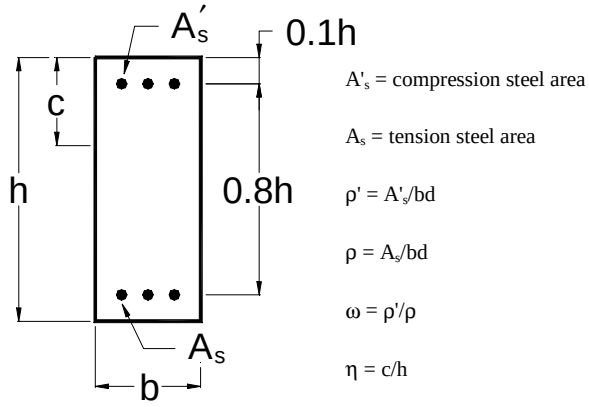

a). A doubly reinforced beam section

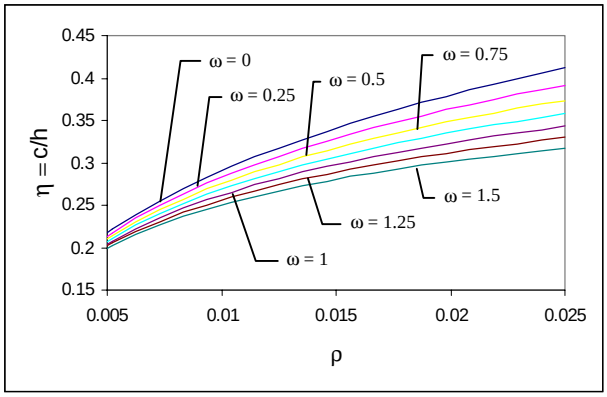

b i). Beam section with concrete strength equals to 20 MPa

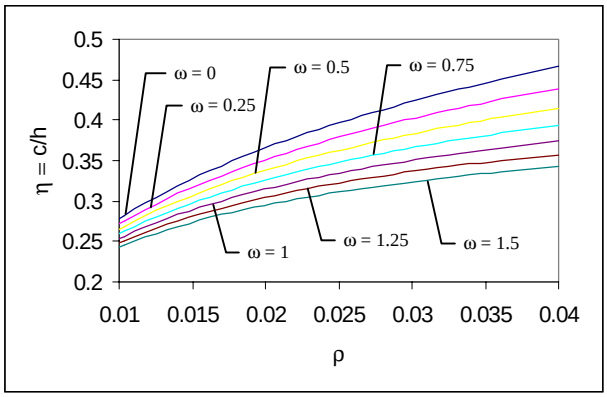

b ii). Beam section with concrete strength equals to 30 MPa

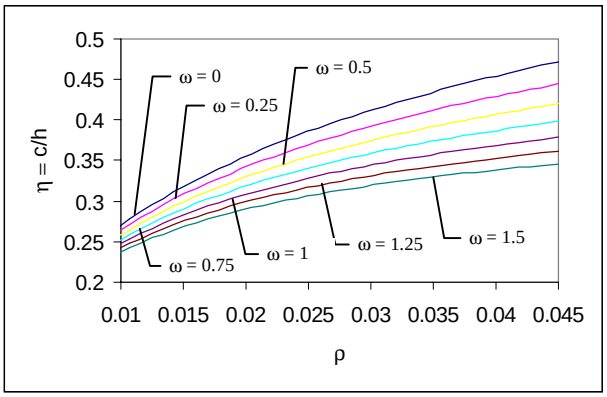

b iii). Beam section with concrete strength equals to 40 MPa

Figure 4. Ratio of neutral axis depth to sectional height of a doubly reinforced concrete beam section.

Compression and tension chords area

The strain profile of a doubly reinforced beam section, see Fig. 5a and the corresponding STM, see Fig. 5c, subjected to identical elastic moment are depicted in Fig. 5b & 5d respectively. In order to capture the member stiffness correctly, two condition should be satisfied. They are:

1. The elastic cracked section neutral axis depth, c, in the beam section is equal to that in the STM.
2. The strain magnitude at the steel tension centroid of the beam section, represented by ε^*_T in Fig. 5b, is identical to that of the tension tie in STM, represented by ε'_T. in Fig. 5d.
3.

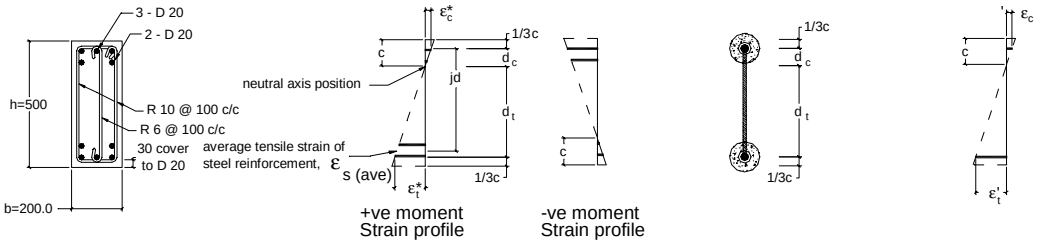

a) Beam cross sectional details

b) Strain profile of the beam section in elastic state

c) Cross section of STM

d) The strain profile of the STM subjected to +ve moment

Figure 5. Strain profile of a doubly reinforced concrete beam section and the corresponding STM.

Assume that the internal lever arm, *jd*, of an actual beam section in the elastic state is approximately equal to 0.9h-c/3, then the moment capacity of the beam section and STM can be given by Eq. 2 & Eq. 3 respectively.

These two equations were then combined based upon the previously stated strain conditions, allowing the STM compressive chord cross-sectional area, A_{cm}, to be computed using Eq 4.

$$M = \frac{\varepsilon_T^* c}{2(d-c)} E_c cb \times \left(0.9h - \frac{c}{3}\right) \tag{2}$$

$$M = \frac{\varepsilon_T' (c - 0.1h)}{(0.9h - c)} E_c A_{cm} \times 0.8h \tag{3}$$

$$A_{cm} = bh \times \frac{\eta^2 (0.9 - 0.33\eta)}{1.6(\eta - 0.1)} \tag{4}$$

where M is the moment capacity of the beam and STM section; d is the effective depth of tension reinforcement measured from the section upper edge and η is the ratio of elastic cracked neutral axis depth to the total section depth (i.e. η = c/h).

The approach used to compute the tension chord cross-sectional area is similar to that previously detailed for the compression chord. Again, the moment capacity was computed for both the beam and STM sections as given in Eq. 5 & Eq. 6, respectively. Again, these two equations were combined according to the previously stated strain conditions, enabling the tension chord cross-sectional area, A_{sm}, to be computed by Eq. 7.

$$M = \varepsilon_T^* E_s A_s \times \left(0.9h - \frac{c}{3}\right) \tag{5}$$

$$M = \varepsilon_T' E_s A_{sm} \times 0.8h \tag{6}$$

$$A_{sm} = A_s \frac{0.9 - 0.33\eta}{0.8} \tag{7}$$

Diagonal compression strut area

An analytical method with experimental verification for determining the area of diagonal strut members is not yet available. Thus, an empirical method was employed here to obtain the member size which is to multiply the perpendicular distance between the diagonal members in STM, l_d,(see Fig. 7) and the beam sectional width, b, together. The inclined angle of diagonal members can be freely chosen according to the suggested limits by CEB-FIP[1978] between the range of 31^o and 59^o. If the diagonal compression strut is situated in the potential plastic hinge zone, it is however advisable to choose the upper angle limit in order to reflect the actual crack patterns.

Transverse tie area

The conventional approach equate the shear strength contribute by transverse reinforcement as:

$$V_s = f_y A_{vs} \, d/s \tag{8}$$

which assumes shear cracks at 45^o to the longitudinal axis having the projected horizontal distance of the crack is equal to the sectional effective depth, d. However, these cracks actually develop with a range of inclined angles in the beam subjected to a combined flexural and shear actions. It is conceivable that the number of stirrups intercept a steep diagonal crack, see Fig. 6a is less than that crossing a flatter one, see Fig. 6b. Since the truss bay length in STM is dictated by the inclined angle of the diagonal compression strut, it is logical that the transverse tie area contributed by shear reinforcement can be computed according to the average bay length, l_b, (see Fig. 7) of the two neighbouring truss bays. The transverse tie area contributed by the concrete was computed based upon the equation suggested by NZS 3101:1995. It follows that the effective area, A_{vm}, of the transverse tie to be used in the mode is:

$$A_{vm} = A_v \frac{l_b}{s} + \frac{(0.07 + 10\rho_w)\sqrt{f_c'}}{f_{vy}} bd \qquad \text{but } 0.08 \le (0.07+10\rho_w) \le 0.2 \tag{9}$$

where A_v is the area of shear reinforcement; s is the spacing of stirrups; ρ_w is the ratio of tension reinforcement to beam effective sectional area; f'_c is the concrete compressive strength and f_{vy} is the tensile strength of shear reinforcement.

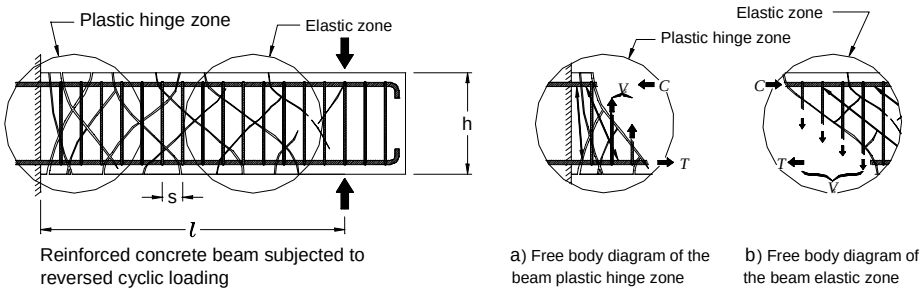

Figure 6. The cracking patterns of a cantilever beam when subjected to cyclic loading.

Member strength

Allowable compressive strength of the compression member used in STM is still a subject of controversy. In this study, the strength of $0.72f'_c$ was adopted for the uniaxial compression chords. This value was selected to correspond with the previously detailed damage factor of 0.85, in addition to an extra 15% strength reduction to represent the average concrete compressive stress in the actual beam section. For the diagonal compression strut located outside the potential plastic hinge zone, compressive strength of $0.68\ f'_c$ was assigned based upon the expected tensile strain induced by transverse steel reinforcement. For the diagonal compression strut inside the plastic hinge zone, compressive strength of $0.34\ f'_c$ was chosen recognising the potential for development of cracks with wide crack width [Schlaich et al., 1987]. For the tension strength of uniaxial tension chords and transverse ties, the measured material strength of steel reinforcement was used in this study.

DESIGN EXAMPLES

In this section the cyclic hysteretic response of three cantilever beam units was modelled using the STM formulation with the suggested procedures. Relevant structural details are listed in Table 1.

Table 1. Structural details of the modelled cantilever beams.

	Beam 1*	Beam 2**	Beam 3***
Sectional width, b (mm)	200	200	228.6
Sectional height, h (mm)	500	500	406.4
Top reinforcing steel area, A'_s (mm^2)	1570.8	1570.8	1140.1
Bottom reinforcing steel area, A_s (mm^2)	1570.8	1005.3	593.8
Transverse reinforcing steel area, A_v (mm^2)	185.4	191.6	126.7
Shear span, l (mm)	1500	1329	1587.5
Stirrup spacing, s (mm)	100	100	88.9
Concrete compressive strength, f'_c (MPa)	33.2	27.7	31.58
Yield strength of longitudinal steel reinforcement, f_y (MPa)	311	280 (top) 298 (bottom)	451.6 (top) 458.5 (bottom)
Yield strength of transverse steel reinforcement, f_{vy} (MPa)	300	300	413.7

* Data extracted from [Fenwick, et al., 1981] test unit beam 1a.
** Data extracted from [Fenwick and Fong, 1979] test unit beam 3a.
*** Data extracted from [Ma et. al., 1976] test unit beam 3.

A feature relevant to the current study is that all three units were doubly reinforced, having top and bottom longitudinal steel reinforcement with minimal cover to the corresponding edges of the section. Also significant is that the shear strength of the tested units was designed to exceed that required by the codes, and use of high ratio

of shear span to effective depth. Notably, all these aspects are commonly found in ductile beam members designed for seismic loading.

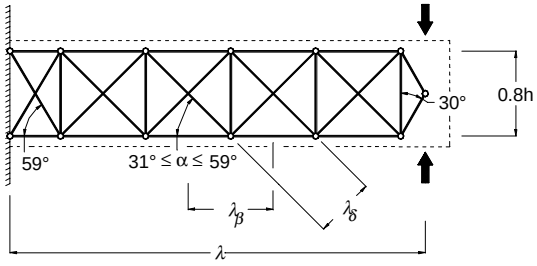

Figure 7. STM layout of a reinforced concrete cantilever beam.

A typical layout of STM used in the nonlinear analysis is illustrated in Fig. 7. It is noteworthy that the diagonal compression strut in the truss bay next to the wall having a steep linclined angle equal to the upper limit suggested by CEB-FIP [1978]. As previously explained, this was to reflect the actual crack patterns of a beam subjected to reversed cyclic loading.

ANALYTICAL RESULTS

The STM nonlinear analytical force-total tip displacement history of the three reinforced concrete cantilever beams are shown in Fig. 8. Results show satisfactory correlation with the experimental observation. The member elastic and plastic stiffness as well as the flexural yield strength were satisfied with good prediction from the models. However, disagreements including the kinks appear on analytical unloading branches and the apparent discrepancy of inelastic unloading stiffness between the analytical responses and the experimental observations are required improvement. Future study will refine material models representing the concrete and the steel

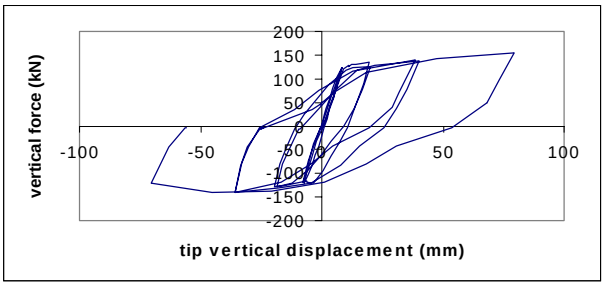

a i) Experimental observed force-tip displacement history of Beam 1.

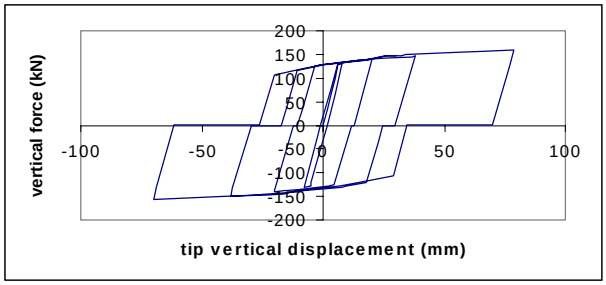

a ii) Analytical force-tip displacement history of Beam 1.

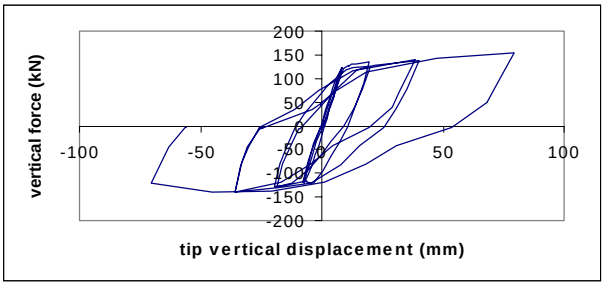

b i) Experimental observed force-tip displacement history of Beam 2

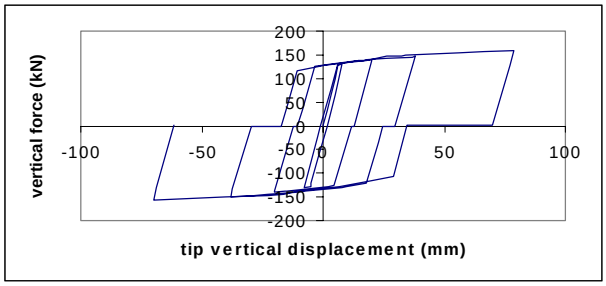

b ii) Analytical force-tip displacement history of Beam 2.

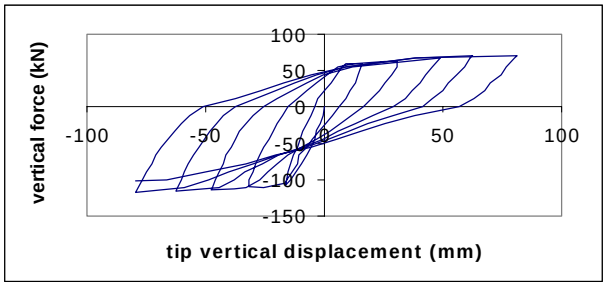

c i) Experimental observed force-tip displacement history of Beam 3

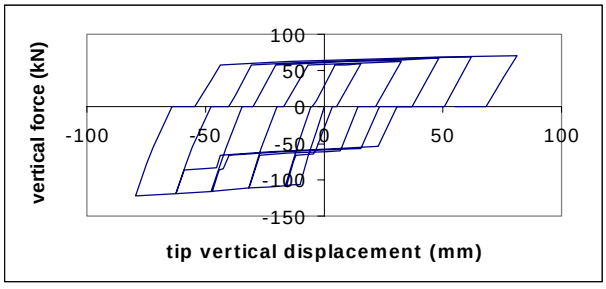

c ii) Analytical force-tip displacement history of Beam 3.

Figure 8. Force-tip displacement history of the reinforced concrete cantilever beams.

reinforcement in order to improve the predicted cyclic hysteretic response by STM.

The experimental records [Fenwick and Fong, 1979] show the proportion of shear to flexural deformation increases with displacement ductility and the number of reversed loading cycles within the identical ductility level. Progress has been made to attempt to capture such ratio change using STM however no conclusive results are available to present in the current research paper.

CONCLUSIONS

1. The current research paper represents a step toward the consistent design approach by developing a simple STM to capture the cyclic hysteretic response of a reinforced concrete cantilever beam with sectional details which are commonly found in seismic design.
2. The suggested procedures, which were developed based upon the internal force distribution of the reinforced concrete structure at the elastic state, proved to adequately predict the reversed cyclic flexural response.
3. Analytical results related to the force-total tip displacement history from the STM satisfactorily correlated to the experimental observations.
4. The model deficiencies, including the kinks in unloading branches and the apparent discrepancy of the inelastic unloading stiffness between analytical results and experimental observation are required further study.

ACKNOWLEDGEMENTS

A research scholarship provided to the primary author by the New Zealand Society for Earthquake Engineering (NZSEE) is gratefully acknowledged.

REFERENCES

1. ACI Committee 445 – Shear and Torsion (1997), *"Strut-and-Tie Bibliography"*, ACI Bibliography No. 16, American Concrete Institute, Farmington Hills, Michigan 48333.
2. Allahabadi, R. and Powell, G. H. (1988), "Drain 2DX User Guide", Report No. EERC-88/06, Earthquake Engineering Research Center, University of California, Berkeley, California.
3. Comité Euro-International du Béton/Fédération International de la Précontrainte (1978), *"CED-FIP Model Code for Concrete Structures"*, 3rd Edition, Paris, 348pp.
4. Douglas, Kim T. (1995), *"Development Of a Reinforced Concrete Plastic Hinge Model"*, Doctoral Dissertation, Department of Civil Engineering, University of Auckland, New Zealand.
5. European Committee for Standardization (CEN) (1991), *"Eurocode 2: Design of concrete structures* Part 1: *General rules and rules for buildings"*, ENV 1992-1-1.
6. Fenwick, R. C. and Fong, A. (1979), *"The Behaviour of Reinforced Concrete Beams under Cyclic loading"*, Report No. 176, Department of Civil Engineering, University of Auckland, New Zealand.
7. Fenwick, R. C. and Thom, C. W. (1982), *"Shear Deformation in Reinforced Concrete Beams Subjected To Inelastic Cyclic Loading"*, Report No. 279, Department of Civil Engineering, University of Auckland, New Zealand.
8. Ma, Shao-Yen M., Bertero, Vitelmo V. and Popov, Egor P. (1976), *"Experimental and Analytical Studies On The Hysteretic Behaviour of Reinforced Concrete Rectangular And T-Beams"*, Report No. EERC 76-2, Earthquake Engineering Research Center, University of California, Berkeley, California.
9. Schlaich, J., Schäfer, K. and Jennewein, M. (1987), *"Toward a Consistent Design of Structural Concrete"*, PCI Journal, Vol. 32, No. 3, pp. 74-150.
10. Standards Association of New Zealand (1995), *"Code of Practice for the Design of Concrete Structures"*, (NZS 3101:1995) Part 2, Wellington.

Tjokrodimuljo, K. (1985), *"Behaviour of Reinforced Concrete Under Cyclic Loading"*, Report No. 374, Dept. of Civil Engineering, University of Auckland, New Zealand.